

Can the morphology of γ -ray emission distinguish annihilating from decaying dark matter?

Céline Boehm,¹ Timur Delahaye,^{1,2} and Joseph Silk³

¹LAPTH, Université de Savoie, CNRS, BP110, F-74941 Annecy-le-Vieux Cedex, France*

²Dipartimento di Fisica Teorica, Università di Torino & INFN - Sezione di Torino, Via Giuria 1, I-10122 Torino, Italia.†

³Astrophysics department, Wilkinson Building, Keble Road, OX1 3RH Oxford, UK‡

(Dated: today)

The recent results from the PAMELA, ATIC, FERMI and HESS experiments have focused attention on the possible existence of high energy cosmic ray e^+e^- that may originate from dark matter (DM) annihilations or decays in the Milky Way. Here we examine the morphology of the γ -ray emission after propagation of the electrons generated by both annihilating and decaying dark matter models. We focus on photon energies of 1 GeV, 10 GeV, 50 GeV (relevant for the FERMI satellite) and consider different propagation parameters. Our main conclusion is that distinguishing annihilating from decaying dark matter may only be possible if the propagation parameters correspond to the most optimistic diffusion models. In addition, we point to examples where morphology can lead to an erroneous interpretation of the source injection energy.

I. INTRODUCTION

Results from recent cosmic ray experiments (PAMELA [1], ATIC[2], FERMI [3], HESS[4]) have raised the question of the origin of an “anomalous” population of high energy positrons in the Milky Way and motivated many studies. Correlation of the positron flux measured by PAMELA with the γ -ray spectrum obtained by FERMI LAT is expected to give insight into the injection energy of the high energy electron and positron (e^+, e^-) population, and should also probe their spatial and energy distribution. In scenarios where high energy e^+, e^- are emitted by dark matter (DM), the spatial and energy distribution of this “additional” cosmic ray population is expected to follow the DM halo distribution at the injection energy $E = E_{inj}$. This implies (assuming a spherical DM halo) that they should be spherically distributed with an energy density that is maximal near the Galactic Centre.

However, this picture could be modified if the high energy e^+, e^- spatially propagate and lose energy in the galaxy owing to inverse Compton and synchrotron losses. As a consequence of propagation, not only will the spatial and energy distributions of the high energy e^+, e^- be modified but their final energy will be smaller than E_{inj} . The γ -ray spectrum obtained after propagation could therefore differ significantly from that obtained at injection.

The issue of the γ -ray flux associated with DM annihilations or decays into leptons has been addressed in several papers. For example, both the γ -ray flux and γ -ray spectrum in decaying and annihilating scenarios have been discussed in ref. [5, 6] but propagation was actually neglected. More recently, the authors of ref.[7] have predicted the expected γ -ray flux in a decaying DM model, taking into account e^+, e^- propagation. Although computation of the flux is important, exploiting its value will be difficult owing to large uncertainties due to astrophysical sources at these energies (Ref.[8]). Other papers have considered specific positions on the sky (e.g. interme-

diated galactic latitudes, [9, 10]), or rely on very large-scale anisotropies ([7]). The work in ref. [11] raised the question of the morphology of the γ -ray emission but mainly focused on the spectrum; however the propagation parameters adopted are not those favoured by MCMC studies ([12]).

The question we raise in this Letter is whether the morphology of the γ -ray emission alone (rather than the flux) can actually help to discriminate between the different DM scenarios. To address this issue, we compute γ -ray maps originating from the interactions of e^+e^- with the Interstellar Radiation Field (ISRF) spectra after propagation. We assume that the dark matter only annihilates or decays into e^+e^- pairs and focus on γ -ray energies that are accessible by the FERMI satellite, namely $E_\gamma = 1, 10, 50$ GeV. We have neglected prompt γ emission which could arise from internal bremsstrahlung because its spectrum is model-dependent, however one should keep in mind that for some models, this emission could modify our conclusions. Given our assumptions, the injection energy of the e^+ and e^- corresponds to either the DM mass m_{dm} or half the DM mass ($E_{inj} = m_{dm}$ or $m_{dm}/2$), depending on whether DM is annihilating or decaying respectively. We will consider three values of the injection energy: $E_{inj} = 100, 500, 1000$ GeV. At given E_{inj} , the comparison between decaying and annihilating scenarios is immediate. In addition, since there are quite large uncertainties in the propagation parameters of cosmic rays, we will use three different sets of parameters referred to as (MIN, MED, MAX) (cf Ref. [13, 14]), which give a fair idea of the related uncertainty. We present difference maps of the γ -ray contributions that highlight how morphology could help discriminate between the competing models.

II. PRODUCING GAMMA-RAY MAPS

To generate these maps, we apply the propagation scheme introduced by [13], modified according to [15, 16] for primary electrons. We compute the halo function \tilde{I} in terms of the electron energy:

$$\tilde{I} = \sum_i \sum_n J_0 \left(\frac{\alpha_i r}{R_{gal}} \right) \times \varphi_n(z) \times e^{\left\{ -\left(\frac{\pi r}{2L} \right)^2 + \frac{\alpha_i^2}{R_{gal}^2} \right\} \lambda_d^2} \times Q_{in} \quad (1)$$

*Electronic address: celine.boehm@cern.ch

†Electronic address: delahaye@lapp.in2p3.fr

‡Electronic address: j.silk1@physics.ox.ac.uk

$E_{inj} = 100\text{GeV}$	parameter	a_{10}	b_{10}	ϵ_{10}	a_2	b_2	ϵ_2
$E_\gamma = 10\text{ GeV}$							
ann	MIN	19	6.5	0.66	7.5	4	0.47
decay	MIN	95	8	0.92	19	4	0.79
ann	MED	10	25	0.31	15	8.5	0.1
decay	MED	126	35	0.72	30.5	15.5	0.49
ann	MAX	54	45.5	0.16	23	21.5	0.07
decay	MAX	179.5	67	0.63	40.5	32.5	0.2

TABLE I: Ellipticity for $E_\gamma = 10\text{ GeV}$ and $E_{inj} = 100\text{ GeV}$ for 0.1 (subscript 10) and 0.5 (subscript 2) of the intensity.

where $Q_{in} = \kappa R_{in}$ is the Fourier-Bessel transform of the source term (with $\kappa = \frac{\mathcal{A}}{\eta} \times (\rho_0/m_{\text{dm}})^\zeta$ and $\mathcal{A} = \sigma v$ the annihilation cross section if $\zeta = 2$ and $\mathcal{A} = \Gamma$ the decay rate if $\zeta = 1$; η is the multiplicity, i.e. = 2 if Majorana particles, 1 otherwise), L is diffusion slab half-thickness, R_{gal} is Galaxy radius and λ_d the propagation length expressed as:

$$\lambda_d = 4 \times K_0 \times \int_{E_{min}}^{E_{inj}} \frac{E^\delta}{b(E)} dE$$

where $b(E)$ is the loss term and K_0, δ the diffusion parameters. Note that in Eq. (1), r, z are cylindrical coordinates and α_i are the roots of the Bessel function J_0 . The gamma ray flux detected at the Earth is given by the integration along the line of sight of the convolution of the electron flux with the gamma emissivity of the electron interacting with the Interstellar Radiation Field (ISRF). The ISRF is mainly made of stellar light which is absorbed and re-emitted in the infrared by galactic dust. We use the model from [17] which can be fitted by a sum of blackbody (BB)-like spectra as in [18]. Although this fit is valid only in the two kpc around the Sun, we expect that only the relative amplitudes associated with each BB vary from one position to another, but the temperatures should remain the same. The emissivity is computed in the same way as the losses in [18], making the approximation that the outgoing photon spectrum is a delta function ([19]) for each blackbody with which the electrons are interacting.

III. RESULTS

We now present the pixelized maps (with a pixel size of 1 square degree) that we have obtained for the different scenarios. Fig. 1 illustrates (for both annihilating and decaying dark matter models) the difference between the propagation patterns that arise by fixing E_{inj} to 100 GeV and considering three gamma ray energies $E_\gamma = 1, 10, 50\text{ GeV}$. As one can see, in both cases, the e^+, e^- which give rise to 1 GeV photons have propagated further than those giving rise to 50 GeV photons. These features are common to all the maps including those obtained for heavier dark matter candidates. Note that the propagation parameters that we have considered to obtain this map correspond to the MED set ($L = 4\text{ kpc}$, $\delta = 0.7$, $K_0 = 0.0112\text{ kpc}^2/\text{Myr}$).

In Fig.2, we have fixed E_γ to 10 GeV and considered three values of E_{inj} (for both annihilating and decaying DM). Interpreting the features for the particular case $E_{inj} = 500\text{ GeV}$ and $E_\gamma = 10\text{ GeV}$ is non-trivial. As can be seen from Table II, because the ISRF is made of more than one BB, γ -emission at 10 GeV can actually be due to more than one electron population. Indeed bright emission at 10 GeV could be due either to electrons of $\sim 20\text{ GeV}$ interacting with UV light or to $\sim 500\text{ GeV}$ electrons interacting with IR light. Hence as seen in Fig.2, the 10 GeV emission is nearly spherical, and could be interpreted either as an injection energy of $\sim 20\text{ GeV}$ or of $\sim 500\text{ GeV}$, leading to very different interpretations concerning the mass of the DM particle. However this degeneracy can be lifted by looking at higher energies, as electrons injected at 20 GeV cannot produce gamma rays of 50 GeV. This threshold effect stresses how important it is to look at different γ -ray energies and to compare the various morphologies in order to understand the properties of the DM.

In the third column, we exhibit the difference between the two normalized maps (decays – annihilations) so as to exhibit the differences of morphology between these two emission models. The negative values at the Galactic Centre confirm that the e^+, e^- from annihilating DM are mainly produced locally and that propagation cannot completely smooth out the contrast with respect to decaying DM electrons and positrons.

BB	$E_\gamma = 1\text{ GeV}$	$E_\gamma = 10\text{ GeV}$	$E_\gamma = 50\text{ GeV}$
CMB	527 GeV	1.7 TeV	3.7 TeV
IR	151 GeV	479 GeV	1.1 TeV
Stellar	49 GeV	155 GeV	348 GeV
UV1	15 GeV	48 GeV	107 GeV
UV2	11 GeV	35 GeV	78 GeV
UV3	6 GeV	18 GeV	40 GeV

TABLE II: Electron energy E_e responsible for the emission of an electron of energy E_γ through inverse Compton scattering on each blackbody component of the ISRF.

In Fig.3, we show the effect of the propagation parameters for $E_{inj} = 1\text{ TeV}$. As is expected, the $e^+ e^-$ diffuse far more for the set of propagation parameters MAX (for which $L = 15\text{ kpc}$) than for MIN. Although it may be possible to constrain decaying versus annihilating DM in the MAX and MED cases, it seems impossible to distinguish these two scenarios in the MIN case. To compare the propagation features between annihilating and decaying scenarios, it is useful to look at the ellipticities ϵ_{10} and ϵ_2 of the γ -emission. To define these quantities, we measure the size of the semi-major axis a_{10} (or a_2) and the semi-minor axis b_{10} (or b_2) of the ellipse that has an intensity of one tenth (or one half) of the maximal intensity. Ellipticity is then defined as $1 - b/a$. The results are summarized in the caption of Fig. 1,2,3 and Table II. Only for larger masses, or in the optimistic case where the sensitivity allows us to measure ϵ_{10} , is discrimination possible, especially for the MAX propagation model.

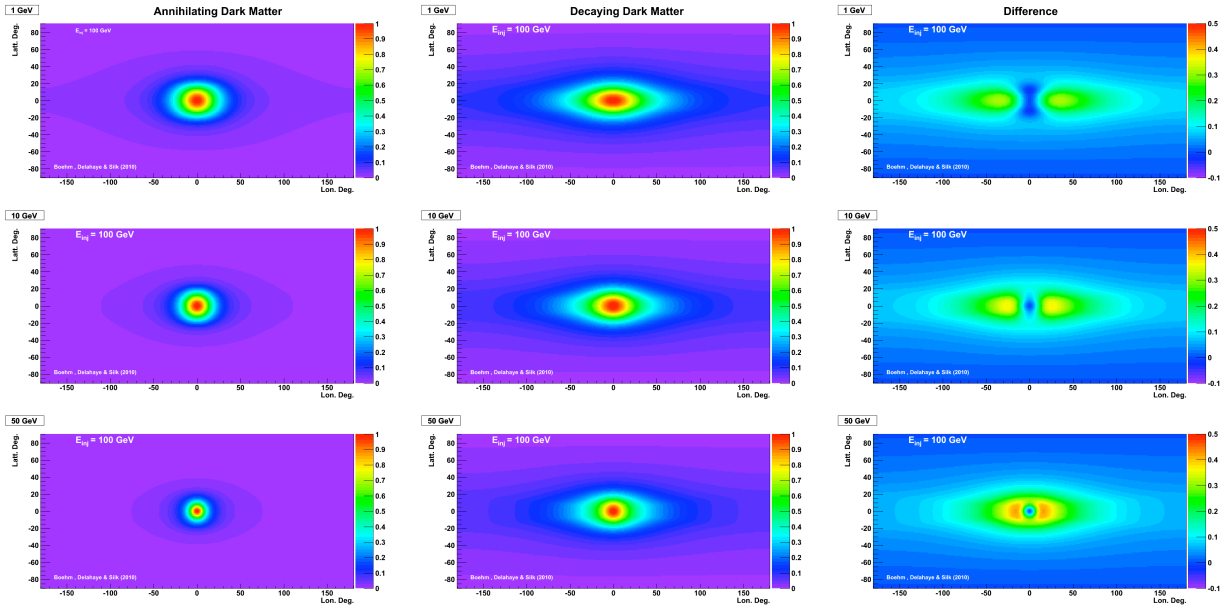


FIG. 1: Annihilating versus decaying DM for $E_{inj}=100$ GeV and $E_\gamma = 1, 10, 50$ GeV. In these figures, fluxes are normalized to the central bin so as to make the comparison of propagation length obvious. Ellipticities at 0.1 of the central bin intensity are equal to $\varepsilon_{10} = 0.41, 0.31, 0.15$ and $\varepsilon_{10} = 0.75, 0.72, 0.68$ for annihilating versus decaying DM respectively.

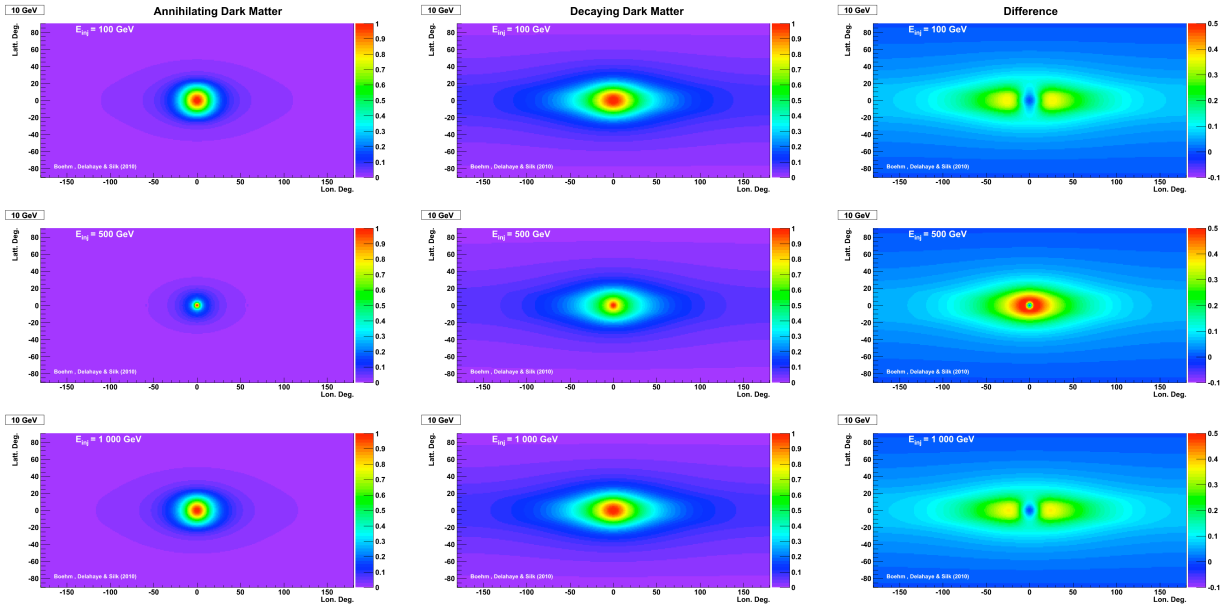


FIG. 2: Annihilating versus decaying DM for $E_\gamma = 10$ GeV and $E_{inj} = 100, 500, 1000$ GeV. Ellipticities at 0.1 of the central bin intensity are equal to $\varepsilon_{10} = 0.31, 0.06, 0.35$ and $\varepsilon_{10} = 0.72, 0.67, 0.72$ for annihilating versus decaying DM respectively.

IV. CONCLUSION

We have generated maps of γ -ray emission associated with e^+, e^- population originating from DM annihilations or decays. We show that propagation is important for both DM scenarios, but although the propagation features differ, they are difficult to distinguish if the propagation parameters correspond to MIN (and perhaps MED) rather than to MAX. This

is, in fact, surprising, as one might have expected these two scenarios, which involve distinct powers of the dark matter density, to differ significantly. Actually, in the MIN case, detection would be extremely challenging since most of the signal would be hidden by galactic sources. In some cases, the IRSF can make the Galactic Centre bright enough to be misinterpreted as e^+e^- with a lower injection energy.

We have verified that changing the energy density of the IRSF

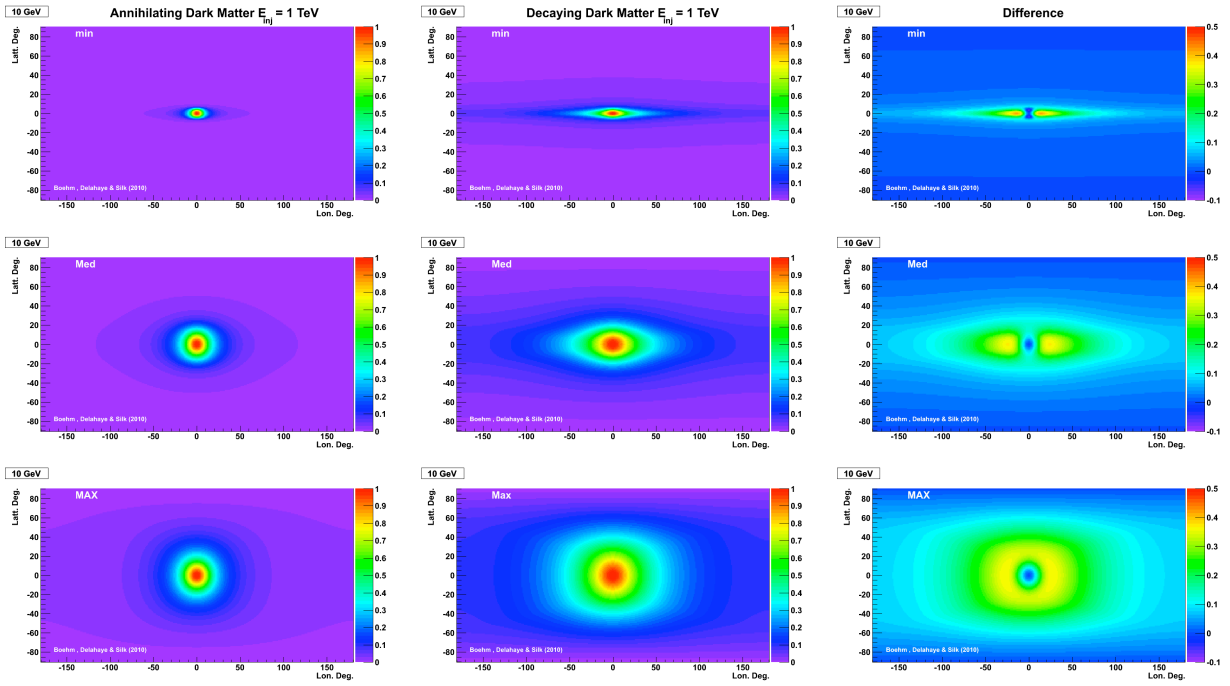


FIG. 3: Annihilating versus decaying DM for $E_{inj} = 1$ TeV and the min and MAX propagation parameters. Ellipticities at 0.1 of the central bin intensity for MIN and MAX are equal to $\epsilon_{10} = 0.67, 0.35, 0.15$ and $\epsilon_{10} = 0.92, 0.72, 0.58$ for annihilating versus decaying DM respectively.

has little effect as the increase of the γ -ray emissivity is partially compensated by the electron density decrease due to increased energy losses. Varying the intensity of the magnetic field within reasonable values has also little impact as synchrotron emission is not the main energy loss term in most cases. In both cases the impact is mainly on the intensity and not on the ellipticity. However a full spatial description of

both the ISRF and the magnetic field could have effects that are beyond the scope of our analytical approach.

We would like to thank P. Salati and A. Fiasson for very useful discussions. and acknowledge fundings from the "low energy electron and positron propagation" PICS.

-
- [1] O. Adriani, G. C. Barbarino, G. A. Bazilevskaia, R. Bellotti, M. Boezio, E. A. Bogomolov, L. Bonechi, M. Bongi, V. Bonvicini, S. Bottai, et al., *Nature (London)* **458**, 607 (2009), 0810.4995.
- [2] J. Chang, J. H. Adams, H. S. Ahn, G. L. Bashindzhagyan, M. Christl, O. Ganel, T. G. Guzik, J. Isbert, K. C. Kim, E. N. Kuznetsov, et al., *Nature (London)* **456**, 362 (2008).
- [3] A. A. Abdo, M. Ackermann, M. Ajello, W. B. Atwood, M. Axelsson, L. Baldini, J. Ballet, G. Barbiellini, D. Bastieri, M. Batteino, et al., *Physical Review Letters* **102**, 181101 (2009), 0905.0025.
- [4] F. Aharonian, A. G. Akhperjanian, U. Barres de Almeida, A. R. Bazer-Bachi, Y. Becherini, B. Behera, W. Benbow, K. Bernlöhr, C. Boisson, A. Bochow, et al., *Physical Review Letters* **101**, 261104 (2008), 0811.3894.
- [5] M. Cirelli, P. Panci, and P. D. Serpico, ArXiv e-prints (2009), 0912.0663.
- [6] M. Cirelli and P. Panci, *Nuclear Physics B* **821**, 399 (2009), 0904.3830.
- [7] L. Zhang, C. Weniger, L. Maccione, J. Redondo, and G. Sigl, ArXiv e-prints (2009), 0912.4504.
- [8] T. Linden and S. Profumo, ArXiv e-prints (2010), 1003.0002.
- [9] G. Bertone, M. Cirelli, A. Strumia, and M. Taoso, *Journal of Cosmology and Astro-Particle Physics* **3**, 9 (2009), 0811.3744.
- [10] S. Profumo and P. Ullio, ArXiv e-prints (2010), 1001.4086.
- [11] M. Regis and P. Ullio, *Phys. Rev. D* **80**, 043525 (2009), 0904.4645.
- [12] D. Maurin, A. Putze, and L. Derome, ArXiv e-prints (2010), 1001.0553.
- [13] D. Maurin, F. Donato, R. Taillet, and P. Salati, *Astrophys. J.* **555**, 585 (2001), arXiv:astro-ph/0101231.
- [14] F. Donato, D. Maurin, P. Salati, A. Barrau, G. Boudoul, and R. Taillet, *Astrophys. J.* **563**, 172 (2001), arXiv:astro-ph/0103150.
- [15] T. Delahaye, R. Lineros, F. Donato, N. Fornengo, and P. Salati, *Phys. Rev. D* **77**, 063527 (2008), 0712.2312.
- [16] T. A. Porter, I. V. Moskalenko, and A. W. Strong, *Astrophys. J. Letters* **648**, L29 (2006), arXiv:astro-ph/0607344.
- [17] T. A. Porter, I. V. Moskalenko, A. W. Strong, E. Orlando, and L. Bouchet, *Astrophys. J.* **682**, 400 (2008), 0804.1774.
- [18] T. Delahaye, J. Lavalley, R. Lineros, F. Donato, and N. Fornengo, ArXiv e-prints (2010), 1002.1910.
- [19] G. R. Blumenthal and R. J. Gould, *Reviews of Modern Physics* **42**, 237 (1970).